Theory and Application of SNR and Mutual Information Matched Illumination Waveforms

RIC A. ROMERO, Member, IEEE

JUNHYEONG BAE, Student Member, IEEE

NATHAN A. GOODMAN, Senior Member, IEEE
University of Arizona

A comprehensive theory of matched illumination waveforms for both deterministic and stochastic extended targets is presented. Design of matched waveforms based on maximization of both signal-to-noise ratio (SNR) and mutual information (MI) is considered. In addition the problem of matched waveform design in signal-dependent interference is extensively addressed. New results include SNR-based waveform design for stochastic targets, SNR-based design for a known target in signal-dependent interference, and MI-based design in signal-dependent interference. Finally we relate MI and SNR in the context of waveform design for stochastic targets.

Manuscript received May 24, 2008; revised June 19 and October 16, 2009; released for publication November 9, 2009.

IEEE Log No. T-AES/47/2/940821.

Refereeing of this contribution was handled by Y. Abramovich.

Authors' address: Dept. of Electrical and Computer Engineering, Naval Postgraduate School, Spanagel Hall, 833 Dyer Rd., Monterey, CA 93943, E-mail: (rnromero@nps.edu).

I. INTRODUCTION

Transmit waveform design is critical to radar system performance. As such, waveform design has a long history and rich literature. However implied in most of the designs is the assumption that targets have infinite wideband response, i.e., point targets. Indeed many advances in radar technology have been based on this assumption. Common waveforms such as phase codes, wideband chirps, and pulse trains are traditionally designed for range resolution, Doppler resolution, and ambiguity considerations. Furthermore no provision is applied to "adaptively" change them while in operation. In fact most adaptive signal and knowledge-based processing algorithms are "receiver-centric." Our focus here is on designing and adapting waveforms that are matched to ensembles of extended targets. When used in a "transmitter-centric" closed-loop radar system, these transmit waveforms can be adaptively modified by exploiting the knowledge learned from the environment through prior received echoes.

The design of matched waveforms has been investigated from both signal-to-noise ratio (SNR) and mutual information (MI) considerations. The optimum waveform for maximizing SNR due to a known target in additive Gaussian noise was first investigated in [1], [2]. The problem of matching a known target response in a signal-dependent interference and additive channel noise was first investigated in [3]. While no closed-form solution was derived, a numerical approach was presented. It was noted here that traditional waveforms, such as linear-FM waveforms, were inferior in SNR performance for extended targets. Unfortunately the work in [3] is not guaranteed to converge to the optimal design [4]. In [5], [6], the technique in [3] was extended to a target-recognition application. Earlier work in signal design for detection and system identification includes the works in [7]–[9]. In addition signal design for clutter rejection was considered in [10], and waveform selection from the point of view of target recognition was considered in [11]. The work of Kay [4] presented optimal signal design for detection of Gaussian point targets in Gaussian clutter.

Considering the problem of estimation, Bell also made a considerable advance by investigating waveforms designed to maximize MI between the received signal and a Gaussian target ensemble [1, 2]. By now, the direct relationship between two measurement metrics: estimation theory's minimum mean square error (MMSE) and information theory's MI in Gaussian channels, is well known [12]. The use of MMSE/MI in designing waveforms was extended for multiple-input multiple-output (MIMO) target recognition and classification applications [13]. The work in [14] used MI-based radar waveform design for multiple extended targets.

In [15], Haykin proposed cognitive radar as a technological solution for performance optimization in resource-constrained and interference-limited environments. Addressing this notion of a closed-loop intelligent radar in our earlier work [16], we introduced a specific cognitive radar platform which utilized the techniques in [1], [2], [5], [6]. Both SNR and MI were used to adaptively modify transmit waveforms for recognition of known targets. It was shown that this closed-loop radar framework can reduce the energy required for identification. In [17], [18], the closed-loop radar strategy was applied to discrimination of target classes rather than a finite ensemble of known targets. Finally in [18], we have presented initial results on designing waveforms that maximize MI in the presence of signal-dependent interference.

From the above discussion, it is clear that two criteria (SNR and MI) have been primary metrics used to design matched waveforms. Furthermore various target and interference paradigms are possible. These paradigms include treating the target as either deterministic or random and treating the interference as either signal-independent (receiver noise) or signal-dependent (clutter). The list below shows possible design paradigms for both SNR-based and MI-based approaches. The list also identifies references relating to previous contributions for each paradigm. This paper presents four new matched waveform contributions: information-theoretic waveform in signal-dependent interference, a new frequency-domain approach to maximizing SNR in signal-dependent clutter, and two SNR-based waveforms that apply to random target ensembles. To the best of our knowledge, these latter two paradigms have not been addressed in the literature. It should be noted that, in the case of maximizing SNR for a known target in signal-dependent clutter, a recent work [19] arrived at a similar frequency-domain approach as our own. Paradigms where we make new waveform design contributions in this paper are denoted by (*) in the list below. For completeness, we derive all the matched waveforms for all cases shown in the list below.

Known Target

1) SNR-based waveform design in signal-dependent interference, [3, 19]. (*)
2) SNR-based waveform design in noise, [1, 2].

Stochastic Target

1) SNR-based waveform design in signal-dependent interference. (*)
2) SNR-based waveform design in noise. (*)
3) MI-based waveform design in signal-dependent interference. (*)
4) MI-based waveform design in noise. [1, 2]

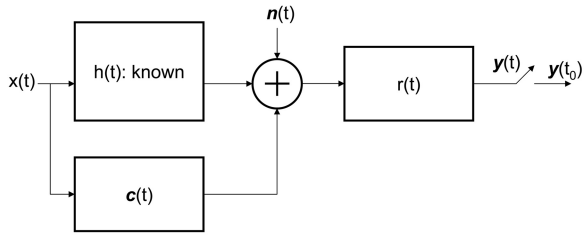

Fig. 1. Known target signal model for SNR-based waveform design.

One consideration in forming practical radar waveforms is the constant modulus constraint, which permits efficient use of the front-end power amplifier(s) [20]. SNR-based waveform designs (in signal-dependent interference) and MI-based waveform designs via an energy constraint presented in this paper resulted in optimal transmit spectra. With proper manipulation of the waveforms in the temporal domain, it should be possible to design constant modulus waveforms that approximate SNR-based or MI-based waveform spectra with some loss of optimality. For example, a recent work [21] introduces a technique for spectrally designed waveforms to have constant envelopes.

This paper is organized as follows. Section II describes the signal models used for the known target case and presents SNR-based matched waveform designs. Section III describes the signal models used for the finite-duration stochastic target case and presents derivations of the matched waveform designs for both SNR-based and MI-based paradigms. Based on the prior section, Section IV relates MI and SNR in the context of waveform design for stochastic targets and describes transmit waveform behavior for both paradigms and how they are related. Section V presents waveform design examples and applications. Section VI concludes the paper.

II. KNOWN-TARGET SIGNAL MODELS AND SNR-BASED WAVEFORM DESIGN

A. Known Target in Signal-Dependent Interference

The case of a known target in signal-dependent interference was first investigated in [3]. It is difficult to arrive at a closed-form solution for this case since the clutter interference depends on the transmit waveform. Instead a numerical algorithm was proposed in [3] that resulted in a finite-duration transmit waveform and receive filter pair. Unfortunately as mentioned earlier, such an approach did not guarantee convergence to an optimum design [4]. Here we revisit the problem and find a frequency-domain expression for the transmit waveform that maximizes SNR.

Fig. 1 shows a block diagram of the signal model used for SNR-based waveform design. Let $h(t)$ be a known complex-valued baseband target impulse response of finite duration T_h and Fourier transform

$H(f)$. Let $r(t)$ be the complex-valued receive filter impulse response and $\mathbf{n}(t)$ be a complex-valued, zero-mean channel noise process with power spectral density (PSD) $S_{nn}(f)$, which is non-zero over the entire waveform bandwidth. Let $\mathbf{c}(t)$ be a complex-valued, zero-mean Gaussian random process representing an interference component, e.g., ground clutter, and characterized by the PSD $S_{cc}(f)$. Let $x(t)$ be the complex-valued baseband transmit waveform with finite-energy, duration T, and Fourier transform $X(f)$. The transmit waveform's energy is

$$E_x = \int_{-\infty}^{\infty} |X(f)|^2 df.$$

Throughout the paper, an italicized E with a subscript denotes an energy value while the nonitalicized E[·] is the expected value operator. As seen in Fig. 1, the signal $\mathbf{y}(t)$ at the output of the receive filter is

$$\mathbf{y}(t) = r(t) * [x(t)*h(t) + x(t)*\mathbf{c}(t) + \mathbf{n}(t)].$$

Let $y_s(t)$ and $\mathbf{y}_n(t)$ be the signal and noise components, respectively, of the output $\mathbf{y}(t)$, which are defined by

$$y_s(t) = r(t) * x(t)*h(t)$$

and

$$\mathbf{y}_n(t) = r(t) * [x(t)*\mathbf{c}(t) + \mathbf{n}(t)].$$

The output signal-to-interference-plus-noise ratio (SINR) at time t_0 is

$$(\text{SINR})_{t_0} \equiv \frac{|y_s(t_0)|^2}{\text{E}[|\mathbf{y}_n(t_0)|^2]}. \tag{1}$$

The SINR can be written as

$$(\text{SINR})_{t_0} = \frac{\left|\int_{-\infty}^{\infty} R(f)H(f)X(f)e^{j2\pi f t_0} df\right|^2}{\int_{-\infty}^{\infty} |R(f)|^2 L(f) df}$$

where

$$L(f) = |X(f)|^2 S_{cc}(f) + S_{nn}(f).$$

SINR can be reexpressed as

$$(\text{SINR})_{t_0} = \frac{\left|\int_{-\infty}^{\infty} R(f)\sqrt{L(f)}\dfrac{H(f)X(f)}{\sqrt{L(f)}}e^{j2\pi f t_0} df\right|^2}{\int_{-\infty}^{\infty} |R(f)|^2 L(f) df}.$$

Applying Schwarz's inequality [22] yields the bound

$$(\text{SINR})_{t_0} \le \frac{\int_{-\infty}^{\infty} |R(f)|^2 L(f) df \int_{-\infty}^{\infty} \dfrac{|H(f)X(f)|^2}{L(f)} df}{\int_{-\infty}^{\infty} |R(f)|^2 L(f) df}.$$

The SINR achieves its maximum of

$$(\text{SINR})_{t_0} = \int_{-\infty}^{\infty} \frac{|H(f)X(f)|^2}{L(f)} df$$

if and only if the matched filter is of the form

$$R(f) = \frac{[kH(f)X(f)e^{j2\pi f t_0}]^*}{|X(f)|^2 S_{cc}(f) + S_{nn}(f)}$$

where k is an arbitrary constant. Assuming that the transmit signal is essentially limited to the bandwidth W, SINR may be written as

$$(\text{SINR})_{t_0} \simeq \int_W \frac{|H(f)|^2 |X(f)|^2}{S_{cc}(f)|X(f)|^2 + S_{nn}(f)} df \tag{2}$$

and the waveform energy constraint may be written as

$$\int_W |X(f)|^2 df \le E_x. \tag{3}$$

The denominator of (2) depends on the transmit waveform; thus the approach of using the eigenfunction solution to a Fredholm equation [1, 2] does not apply easily [3]. Instead we recognize that the transmit waveform is constrained according to (3) and that the integration kernel of (2) is concave. This leads to use of the Lagrangian multiplier technique, which yields a solution in the form of

$$|X(f)|^2 = \max[0, B(f)(A - D(f))] \tag{4}$$

where $B(f)$ and $D(f)$ are

$$B(f) = \frac{\sqrt{|H(f)|^2 S_{nn}(f)}}{S_{cc}(f)} \tag{5}$$

and

$$D(f) = \sqrt{\frac{S_{nn}(f)}{|H(f)|^2}} \tag{6}$$

respectively, and A is a constant determined by the energy constraint

$$\int_W \max[0, B(f)(A - D(f))] df \le E_x.$$

The derivation of (4) is shown in Appendix I. For a given E_x, once A is found the SINR is calculated by substituting (4) into (2).

The complex-valued transmit waveform that maximizes SINR has a frequency spectrum obtained by performing the waterfilling operation [23] on the function $B(f)(A - D(f))$. While (4) is indeed the transmit waveform spectrum that maximizes the SINR, important observations must be made. First unless the bandwidth W is infinite and the resulting spectrum contains no zero-energy bands of finite width, by the Paley-Wiener Theorem, the waveform defined by (4) cannot be time limited [24], which is an original assumption placed on the waveform design. That the resulting waveform is not time limited is a fundamental limitation of defining waveforms via frequency-domain waterfilling. In some cases the resulting waveform may be approximately limited to the desired time interval; however, even this approximation is not guaranteed in general. Fortunately it is possible to obtain a finite-duration waveform that closely approximates the optimum waveform. For example, we can use finite impulse response (FIR) filter design techniques to find a time

limited waveform that approximates the optimum frequency spectrum in the least-squares sense. Second we now observe the importance of restricting $S_{cc}(f)$ to be positive within the bandwidth W, since it ensures that (5) is always defined. Finally we note that the numerical search necessary to find the correct solution to (4) is a one-dimensional search over the parameter A.

B. Known Target in Noise

In the special case of a clutter-free environment, i.e., $\mathbf{c}(t) = 0$, the output $\mathbf{y}(t)$ is

$$\mathbf{y}(t) = r(t) * [x(t) * h(t) + \mathbf{n}(t)].$$

Thus the received signal and noise components are

$$y_s(t) = x(t) * h(t) * r(t)$$

and

$$\mathbf{y}_n(t) = r(t) * \mathbf{n}(t)$$

respectively.

Since clutter is absent we have the special case of a deterministic target in additive noise. The optimum transmit waveform and receive filter that maximize SNR for real signals while conforming to a transmit energy constraint is due to Bell [1, 2]. With $S_{cc}(f) = 0$, the receive filter is reduced to

$$R(f) = \frac{[kH(f)X(f)e^{j2\pi f t_0}]^*}{S_{nn}(f)}$$

and the SINR expression in (2) reduces to

$$(\mathrm{SNR})_{t_0} = \int_{-\infty}^{\infty} \frac{|H(f)X(f)|^2}{S_{nn}(f)} df. \tag{7}$$

The complex-valued $x(t)$ with finite duration T that optimizes (7) within the energy constraint is defined by

$$\lambda_{\max} \check{x}(t) = \int_{-T/2}^{T/2} \check{x}(\tau) M(t-\tau) d\tau \tag{8}$$

where $M(t)$ is

$$M(t) = \int_{-\infty}^{\infty} \frac{|H(f)|^2}{S_{nn}(f)} e^{j2\pi f t} df$$

and $\check{x}(t)$ is the eigenfunction corresponding to the largest eigenvalue ($\lambda_{\max}$) of this kernel. The resulting SNR is

$$(\mathrm{SNR})_{t_0} = \lambda_{\max} E_x. \tag{9}$$

In summary, the transmit waveform $x(t)$ that maximizes SNR for a known target in additive noise is the eigenfunction corresponding to the maximum eigenvalue of the kernel $M(t)$, and the SNR is just the product of this eigenvalue and the energy in the transmit waveform. In the case where the noise is white, the kernel $M(t)$ becomes

$$M(t) = \frac{1}{N_0} \int_{-\infty}^{\infty} |H(f)|^2 e^{j2\pi f t} df.$$

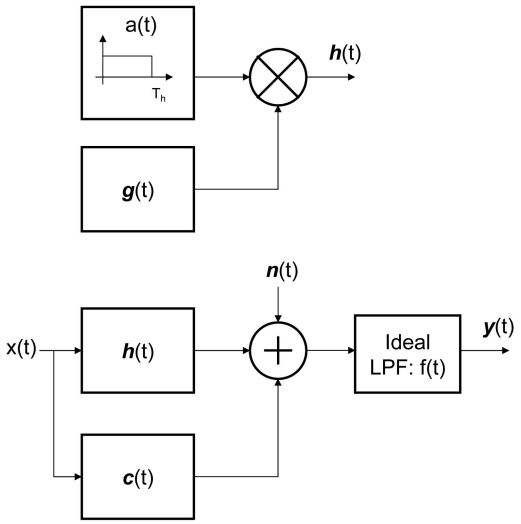

Fig. 2. Top panel: Signal model for finite-duration random target. Bottom panel: Signal model for finite-duration random target in signal-dependent interference.

Thus when the additive noise is white, the kernel $M(t)$ is proportional to the inverse Fourier transform of the energy spectrum of the deterministic target. Finally the $\check{x}(t)$ in (8) is noncausal, but according to (9), a phase shift does not affect the SNR. Therefore the waveform can be made causal by applying the proper time delay [1].

III. FINITE-DURATION STOCHASTIC TARGET AND WAVEFORM DESIGN

In [1], [2], an extended target was modeled as a random process in order to derive a matched waveform that maximized the mutual information between the random target and the received echo. As opposed to an infinite-time process, it was postulated that this stochastic target $\mathbf{h}(t)$ is a finite-energy finite-duration process where T_h is the time duration where most of the target energy resides. The output SNR expression in (1) is inappropriate for application to a scenario with this type of target; thus another SNR definition is needed but will need to wait until we formalize a proper model description for an extended target that is random and exists only in a finite time interval.

A. The Finite-Duration Stochastic Target Model

We formalize the definition of a stochastic extended target by building upon the target model initially introduced in [1], [2]. The random extended target model is a process that can be considered stationary within the interval $[0, T_h]$ but is zero outside this interval. For SNR-based waveform design, the process does not need to be Gaussian. A signal of this nature can be constructed from elementary signal models. Fig. 2 (top panel) shows how such a process is created, where $\mathbf{g}(t)$ is a complex wide-sense stationary process with some PSD and $a(t)$ is a

rectangular window function of duration T_h. It is clear that the product $\mathbf{h}(t) = a(t)\mathbf{g}(t)$ is a finite-duration random process having support only in $[0,T_h]$. Furthermore, since $\mathbf{g}(t)$ is wide-sense stationary, $\mathbf{h}(t)$ is locally stationary within $[0,T_h]$. This unique random process has been mathematically explored in [25], [26].

Since $\mathbf{h}(t)$ is a finite-energy process, we can assume that any realization of $\mathbf{h}(t)$ is integrable, i.e., any sample function $h(t)$ has a Fourier transform $H(f)$ such that

$$E_h = \int_{T_h} |h(t)|^2 dt = \int_{-\infty}^{\infty} |H(f)|^2 df.$$

We can also obtain the time-averaged power P_h within the interval $[0,T_h]$ as suggested in [27], which is given by

$$P_h = \frac{1}{T_h}\int_{T_h} |h(t)|^2 dt = \frac{1}{T_h}\int_{-\infty}^{\infty} |H(f)|^2 df.$$

One may consider $H(f)$ to be a sample realization of a random transfer function $\mathbf{H}(f)$, where $\mathbf{H}(f)$ is the Fourier transform counterpart of $\mathbf{h}(t)$. Next consider the energy of $\mathbf{h}(t)$ or $\mathbf{H}(f)$ averaged over the ensemble of target realizations. This ensemble-averaged energy can be calculated by

$$\bar{E}_{\mathbf{h}} = \int_{T_h} \mathrm{E}[|\mathbf{h}(t)|^2]dt = \int_{-\infty}^{\infty} \mathrm{E}[|\mathbf{H}(f)|^2]df. \quad (10)$$

Note that (10) is an energy quantity, not power; hence $\mathrm{E}[|\mathbf{H}(f)|^2]$ is not a PSD as would typically be used for characterizing a random process. Instead the ensemble's average power, defined only in the interval $[0,T_h]$, can be obtained through time averaging by

$$\bar{P}_{\mathbf{h}} = \frac{1}{T_h}\int_{T_h} \mathrm{E}[|\mathbf{h}(t)|^2]dt = \frac{1}{T_h}\int_{-\infty}^{\infty} \mathrm{E}[|\mathbf{H}(f)|^2]df. \quad (11)$$

Observing (10)–(11), an energy spectral density (ESD) can be defined as

$$\xi_H(f) = \mathrm{E}[|\mathbf{H}(f)|^2].$$

Furthermore if the mean of the random transfer function is

$$\mu_H(f) = \mathrm{E}[\mathbf{H}(f)]$$

then we can define

$$\sigma_H^2(f) = \mathrm{E}[|\mathbf{H}(f) - \mu_H(f)|^2] \quad (12)$$

as the variance of $\mathbf{H}(f)$, called the energy spectral variance (ESV) [1, 2]. We assume in this paper that $\mu_H(f) = 0$, in which case the ESD and ESV functions are equal. The ESV describes the average energy of a finite-duration, zero-mean process in the same sense that a PSD describes the average power of an infinite-duration, wide-sense stationary process. From (11), (12), and the zero-mean assumption, we define

$$\Upsilon_H(f) = \frac{\sigma_H^2(f)}{T_h} = \frac{\mathrm{E}[|\mathbf{H}(f)|^2]}{T_h} \quad (13)$$

where $\Upsilon_H(f)$ will be known as the power spectral variance (PSV). By (11),

$$\bar{P}_{\mathbf{h}} = \int_{-\infty}^{\infty} \frac{\mathrm{E}[|\mathbf{H}(f)|^2]}{T_h} df = \int_{-\infty}^{\infty} \Upsilon_H(f) df$$

that is, the time-averaged power $\bar{P}_{\mathbf{h}}$ of a finite-duration process is described by its PSV. Care must be exercised so as not to confuse $\Upsilon_H(f)$ as a PSD. Since $\mathbf{h}(t)$ is not a power process, a PSD does not apply. Indeed the Wiener-Khintchine Theorem [28] defines a PSD only for random processes where the autocorrelation exists in the interval $[-\infty,\infty]$. Since $\Upsilon_H(f)$ is a time-scaled version of an ESV, it contains the same information as the ESV except that it conveys the critical power content in $[0,T_h]$. Since $\mathbf{h}(t)$ is stationary within the interval $[0,T_h]$, $\mathrm{E}[|\mathbf{h}(t)|^2]$ is constant in that interval, and thus, the time-averaged power is

$$\bar{P}_{\mathbf{h}} = \mathrm{E}[|\mathbf{h}(t)|^2] = \int_{-\infty}^{\infty} \Upsilon_H(f) df. \quad (14)$$

Since the transmit waveform convolves with the target response, a linear system model has to be developed for finite-time duration processes. Let $\mathbf{z}(t)$ be the random output that results from convolving waveform $x(t)$ with a random target $\mathbf{h}(t)$. Given a particular realization $h(t)$ with Fourier transform $H(f)$, we have

$$z(t) = x(t)(t) \leftrightarrow Z(f) = X(f)H(f).$$

Thus

$$\mathrm{E}[|\mathbf{z}(t)|^2] = \mathrm{E}[|x(t)*\mathbf{h}(t)|^2]$$

and

$$\mathrm{E}[|\mathbf{Z}(f)|^2] = \mathrm{E}[|X(f)|^2|\mathbf{H}(f)|^2]. \quad (15)$$

It is important to note here that the quantity $\mathrm{E}[|\mathbf{z}(t)|^2]$ has support on the interval $[0,T+T_h]$ but is not constant within that interval. Unlike $\mathrm{E}[|\mathbf{h}(t)|^2]$, which was formed by multiplying a true stationary random process with a rectangular window, the quantity $\mathrm{E}[|\mathbf{z}(t)|^2]$ results from the convolution of a finite-duration random impulse response with a finite-duration waveform. At any given time within $[0,T+T_h]$, the expected output power depends on the particular part of the transmit waveform that overlaps the impulse response. For example, clearly the convolution has ramp up and ramp down periods where $\mathrm{E}[|\mathbf{z}(t)|^2]$ changes with time. Thus $\mathrm{E}[|\mathbf{z}(t)|^2]$ is nonstationary within its support interval, and a constant average power that is valid for all times in the interval cannot be defined. In other words, a relationship analogous to (14) cannot be defined for the convolution output. This fact will force approximations to be made when designing waveforms for stochastic targets. It is reasonable to define an ESV from (15) for the output random

process according to

$$\sigma_Z^2(f) = |X(f)|^2 \sigma_H^2(f). \tag{16}$$

Furthermore from (13) and (16), we can define a time-averaged power spectral variance according to

$$\Upsilon_Z(f) = \frac{\sigma_Z^2(f)}{T_z} = \frac{|X(f)|^2 \sigma_H^2(f)}{T_z} = \alpha |X(f)|^2 \Upsilon_H(f) \tag{17}$$

where $T_z = T + T_h$ and $\alpha = T_h/T_z$.

B. SNR-Based Waveform Design for Stochastic Target in Signal-Dependent Interference

Returning to the need for a signal model and SNR expression valid for stochastic targets, we now consider the bottom panel of Fig. 2, which depicts a signal model for stochastic targets to be used for both SNR- and MI-based designs. Let the extended stochastic target be $\mathbf{h}(t)$. Let $x(t)$ be the finite-energy waveform to be designed with finite duration T. Let $\mathbf{n}(t)$ be the zero-mean receiver noise process with PSD $S_{nn}(f)$ that is positive in the signal bandwidth W (i.e., the frequency band $[-W/2, W/2]$). The signal-dependent interference component $\mathbf{c}(t)$ is again a zero-mean random process with PSD $S_{cc}(f)$ that is positive in the bandwidth W. As in [1], the ideal lowpass filter with duration T_f is an acknowledgment that the signals of interest are practically bandlimited and will not affect derivation. We first consider the expressions that result if the target process is a true Gaussian random process $\mathbf{g}(t)$. We then use the notion of spectral variance developed earlier to obtain an approximate expression for SNR. For a true stochastic signal $\mathbf{g}(t)$ with PSD $S_{gg}(f)$ in noise $\mathbf{n}(t)$, the local SNR [29] is given by

$$\mathrm{SNR}_{\mathrm{local}} = \int_{-\infty}^{\infty} R_{\mathrm{SNR}}(f) df = \int_{-\infty}^{\infty} \frac{S_{gg}(f)}{S_{nn}(f)} df \tag{18}$$

where $R_{\mathrm{SNR}}(f) = S_{gg}(f)/S_{nn}(f)$ will now be termed as the SNR spectral density. For a true random target convolved with a transmit waveform in signal-dependent interference, the SINR spectral density is given by

$$R_{\mathrm{SINR}}(f) = \frac{S_{gg}(f)|X(f)|^2}{|X(f)|^2 S_{cc}(f) + S_{nn}(f)}. \tag{19}$$

Since the output is stationary in any observation interval, the integrated SINR in measurement interval T_o is given by

$$\mathrm{SINR} = T_o \int_{-\infty}^{\infty} \frac{S_{gg}(f)|X(f)|^2}{|X(f)|^2 S_{cc}(f) + S_{nn}(f)} df. \tag{20}$$

Since the target $\mathbf{h}(t)$ is of finite duration T_h, we approximate (20) using the stochastic extended target model via the spectral variance functions. With T_f negligible, the output $\mathbf{y}(t)$ has a convolution interval of $T_y = T + T_h$. Replacing a true PSD with the PSV of (17) and observing $\mathbf{y}(t)$ in its interval T_y, we modify (20) to define an SINR quantity valid for a finite-time duration extended target in signal-dependent interference given by

$$\mathrm{SINR} = T_y \int_{-\infty}^{\infty} \frac{\alpha \Upsilon_H(f)|X(f)|^2}{|X(f)|^2 S_{cc}(f) + S_{nn}(f)} df \tag{21}$$

where $\alpha = T_h/T_y$. The scaling α reflects the fact that the convolution output of the finite-duration target and the transmit waveform is only stationary for a finite window of time. The SINR simplifies to

$$\mathrm{SINR} = \int_{-\infty}^{\infty} \frac{\sigma_H^2(f)|X(f)|^2}{|X(f)|^2 S_{cc}(f) + S_{nn}(f)} df.$$

For a waveform with energy concentrated in the band $[-W/2, W/2]$, the SINR equation to be maximized under the energy constraint of (3) is now given by

$$\mathrm{SINR} \simeq \int_W \frac{\sigma_H^2(f)|X(f)|^2}{S_{cc}(f)|X(f)|^2 + S_{nn}(f)} df. \tag{22}$$

Owing to the concavity of the kernel in (22), we again apply the Lagrangian multiplier technique. Maximization of (22) with respect to $|X(f)|^2$ leads to the optimum waveform spectrum described by

$$|X(f)|^2 = \max[0, B(f)(A - D(f))]. \tag{23}$$

where $B(f)$ and $D(f)$ are described by

$$B(f) = \frac{\sqrt{\sigma_H^2(f) S_{nn}(f)}}{S_{cc}(f)} \tag{24}$$

and

$$D(f) = \sqrt{\frac{S_{nn}(f)}{\sigma_H^2(f)}} \tag{25}$$

respectively, and A is a constant determined by the energy constraint

$$\int_W \max[0, B(f)(A - D(f))] df \le E_x.$$

Note the similarity between (23)–(25) and (4)–(6). The only difference is that the energy spectrum $|H(f)|^2$ for the deterministic target has been replaced by the ESV $\sigma_H^2(f)$ of the random target ensemble. Thus the end result seems intuitively satisfying.

For $T_h \gg T$, $\alpha \to 1$, and $\Upsilon_H(f) \to S_{gg}(f)$, the SINR spectral density converges to that of (19). The derivation of (4), which is shown in Appendix I can also be applied to derive (23). Moreover issues associated with the fact that the waveform defined by (23) is not strictly time limited were already discussed in Section IIA. The resulting SINR is defined in (22).

C. SNR-Based Waveform Design for Stochastic Target in Noise

In the special case of a clutter-free environment, i.e., $\mathbf{c}(t) = 0$, the SNR is given by

$$\text{SNR} = \int_{-\infty}^{\infty} \frac{\sigma_H^2(f)|X(f)|^2}{S_{nn}(f)} df. \tag{26}$$

Defining

$$G(f) = \frac{\sigma_H^2(f)}{S_{nn}(f)}$$

(26) is simply

$$\text{SNR} = \int_{-\infty}^{\infty} G(f)|X(f)|^2 df. \tag{27}$$

We desire to maximize (27) using a finite-duration, energy-constrained $x(t)$, which is obtained from the solution to the Fredholm equation given by

$$\lambda_{\max}\check{x}(t) = \int_{-T/2}^{T/2} \check{x}(\tau) R_g(t-\tau) d\tau \tag{28}$$

where the kernel $R_g(t)$ is

$$R_g(t) = \int_{-\infty}^{\infty} G(f) e^{j2\pi f t} df.$$

Equation (28) is easily derived using [1, pp. 1584–85] but with the proper modifications. For white noise, $R_g(t)$ becomes

$$R_g(t) = \frac{1}{N_0} \int_{-\infty}^{\infty} \sigma_H^2(f) e^{j2\pi f t} df.$$

Thus ignoring the scaling factor $1/N_0$, the transmit waveform that maximizes the SNR for a random extended target in white noise is the eigenfunction corresponding to the maximum eigenvalue of the complex-valued target kernel function $R_g(t)$. Moreoever the target kernel function is the inverse Fourier transform of the random target's ESV function. The resulting SNR is

$$\text{SNR} = \lambda_{\max} E_x.$$

Finally we again note the similarity between (28) and the analogous results for a deterministic target in (8).

D. MI-Based Waveform Design for Stochastic Target in Signal-Dependent Interference

Consider again the signal model from the bottom panel of Fig. 2. We are interested in the mutual information between the measurement $\mathbf{y}(t)$ and target ensemble $\mathbf{h}(t)$ given a transmit signal $x(t)$, i.e., $I(\mathbf{y}(t);\mathbf{h}(t) \mid x(t))$. We initially investigated waveform design for the case of a stochastic target in signal-dependent interference in [18] where it was assumed that $T \gg T_h$, $T \gg T_f$, and $T_y \approx T$ [1, 2]. We reconsider the problem in terms of the spectral variance functions defined above and with a stronger treatment of the finite-duration target assumption.

As in the case of the SNR-based derivation, we first consider the mutual information that would result if the target process were a true Gaussian random process $\mathbf{g}(t)$. Since T_f is negligible, we again ignore the effect of the ideal lowpass filter. The received output is given by

$$\mathbf{y}(t) = \mathbf{y}_s(t) + \mathbf{y}_n(t) = x(t) * \mathbf{g}(t) + x(t) * \mathbf{c}(t) + \mathbf{n}(t)$$

where $\mathbf{y}_s(t)$ with PSD $S_Y(f)$ and $\mathbf{y}_n(t)$ with PSD $S_N(f)$ are the signal and interference portions of the output. Then the information rate is

$$\begin{aligned} &\dot{I}(\mathbf{y}(t);\mathbf{g}(t) \mid x(t)) \\ &\quad = \int_W \ln\left[1 + \frac{S_Y(f)}{S_N(f)}\right] df \\ &\quad = \int_W \ln\left[1 + \frac{|X(f)|^2 S_{gg}(f)}{S_{nn}(f) + |X(f)|^2 S_{cc}(f)}\right] df. \end{aligned} \tag{29}$$

Unlike in the case of SNR-based models, it should be noted that the clutter $\mathbf{c}(t)$ is necessarily Gaussian. If the clutter were non-Gaussian, a closed-form expression for the MI rate may not exist. Additionally the true MI rate may not only depend on the second-order statistics, and as such, the MI rate will not lend itself to a convenient expression in terms of the target, clutter, and noise PSDs. In this case any MI-based waveform design based on (29) will be suboptimal in terms of mutual information. Returning to the Gaussian assumption on target, clutter, and noise, the entropy of the target process $\mathbf{g}(t)$ would be infinite (consider the number of time samples necessary to represent a realization of $\mathbf{g}(t)$) such that observing $\mathbf{y}(t)$ for a finite amount of time would yield no quantifiable reduction in the uncertainty of $\mathbf{g}(t)$.

For a finite-duration target $\mathbf{h}(t)$, the initial entropy is finite, but it is not valid to define a PSD. The ESV and PSV of the signal portion of the output are given by

$$\sigma_Y^2(f) = |X(f)|^2 \sigma_H^2(f)$$

and

$$\Upsilon_Y(f) = \frac{\sigma_Y^2(f)}{T_y} \tag{30}$$

where $T_y = T + T_h$ is the duration of the convolution output. Replacing $S_Y(f)$ in (29) with the time-averaged PSV of (30), an approximate information rate can be defined as

$$\begin{aligned} &\dot{I}(\mathbf{y}(t);\mathbf{h}(t) \mid x(t)) \\ &\quad = \int_W \ln\left[1 + \frac{|X(f)|^2 \sigma_H^2(f)}{T_y\{S_{nn}(f) + |X(f)|^2 S_{cc}(f)\}}\right] df. \end{aligned} \tag{31}$$

In reality due to the nonstationary nature of $\mathbf{y}(t)$, the information rate is not uniform on the interval $[0, T_y]$ as (31) would seem to indicate. In effect we

have time-averaged the information rate over the time support of $\mathbf{y}(t)$.

Another potential issue is that (29) is valid only when different samples of the random target's transfer function are uncorrelated Gaussian random variables. In this case, the samples are also independent, and the mutual information due to multiple frequency components can be summed. In the limit as the separation between frequency-domain samples goes to zero, summation becomes integration, which results in (29). However, similar to what was observed in the SNR-based derivations for random targets, allowing arbitrarily close frequency coefficients to be uncorrelated corresponds to allowing the target to be infinite in time duration. Thus applying (31) to finite-duration targets involves two related approximations: substituting a time-averaged PSV for a true PSD and ignoring the correlation between closely-spaced frequency coefficients. Recall that we used the former in our SNR-based derivation. Using the PSV of the signal portion of the output and observing the output in T_y, the approximate mutual information is

$$\begin{aligned}\mathrm{MI} &= I(\mathbf{y}(t);\mathbf{h}(t) \mid x(t)) \\ &= T_y \int_W \ln\left[1 + \frac{|X(f)|^2\sigma_H^2(f)}{T_y\{S_{nn}(f) + |X(f)|^2 S_{cc}(f)\}}\right] df \\ &= T_y \int_W \ln\left[1 + \alpha\left\{\frac{|X(f)|^2\Upsilon_H(f)}{S_{nn}(f) + |X(f)|^2 S_{cc}(f)}\right\}\right] df.\end{aligned} \tag{32}$$

Insofar as we are willing to take the analogy between a true signal portion PSD $S_Y(f)$ and a time-averaged PSV $\Upsilon_Y(f)$, the bracketed term in (32) is analogous to the corresponding term in (29). The additional factor $\alpha = T_h/T_y$ is intuitive in that it accounts for the fact that the output is not stationary in T_y as was noticed in the SNR-based design. In the limit as $T_h \to \infty$, $\mathbf{h}(t)$ becomes the true random process $\mathbf{g}(t)$, $\alpha \to 1$, and the integral in (32) converges to (29).

Subject to the approximations that have been fully discussed above, we now wish to maximize the mutual information $I(\mathbf{y}(t);\mathbf{h}(t) \mid x(t))$ in (32) with respect to $|X(f)|^2$ while conforming to the energy constraint in (3). Despite the signal-dependent interference term in (32), the function within the integral is easily confirmed to be concave. The Lagrangian multiplier technique is invoked, which leads to the waterfilling waveform described by

$$|X(f)|^2 = \max\left[0, -R(f) + \sqrt{R^2(f) + S(f)(A - D(f))}\right] \tag{33}$$

where

$$D(f) = \frac{S_{nn}(f)}{\alpha\Upsilon_H(f)} \tag{34}$$

$$R(f) = \frac{S_{nn}(f)(2S_{cc}(f) + \alpha\Upsilon_H(f))}{2S_{cc}(f)(S_{cc}(f) + \alpha\Upsilon_H(f))} \tag{35}$$

and

$$S(f) = \frac{S_{nn}(f)\alpha\Upsilon_H(f)}{S_{cc}(f)(S_{cc}(f) + \alpha\Upsilon_H(f))}. \tag{36}$$

The constant A is determined by the energy constraint

$$\int_W \max\left[0, -R(f) + \sqrt{R^2(f) + S(f)(A - D(f))}\right] df \le E_x.$$

Once $|X(f)|^2$ is found, the mutual information is easily calculated from (32). The derivation of (33) is shown in Appendix II. As we observed for SNR-based waveform design, defining a waveform's spectrum via waterfilling may lead to conditions that do not satisfy the Paley-Wiener constraint for causality. Hence the time limited constraint may be violated, but an approximate finite-duration waveform is usually possible.

While (33) will be used in the subsequent results section, it is somewhat hard to acquire an intuition of the waveform it describes. To gain further intuition, we apply a first-order Taylor approximation to

$$Q(f) = -R(f) + \sqrt{R^2(f) + S(f)(A - D(f))}.$$

The approximation yields

$$\tilde{Q}(f) = B(f)(A - D(f))$$

where $B(f)$ is

$$B(f) = \frac{\alpha\Upsilon_H(f)}{2S_{cc}(f) + \alpha\Upsilon_H(f)}. \tag{37}$$

Thus the transmit waveform is approximated by

$$|\tilde{X}(f)|^2 = \max[0, B(f)(A - D(f))] \tag{38}$$

where A still controls the waveform's energy. The approximate maximum mutual information can then be calculated by substituting $|\tilde{X}(f)|^2$ in (32). It is clear that if $S_{cc}(f) = 0$, then (37) goes to unity. For the case where clutter is non-zero, $B(f)$ is a clutter-dependent factor that modifies the waterfilling operation. To see its effect, realize that $B(f)$ takes on nonnegative real values between 0 and 1. When the clutter spectrum is zero, the clutter factor becomes one and has no effect. When the clutter factor is non-zero, each frequency component in $A - D(f)$ is weighted depending on the clutter spectrum. As clutter becomes strong at certain frequencies, the clutter factor $B(f)$ goes to zero at those frequencies, and no waveform energy is wasted on those frequencies.

E. MI-Based Waveform Design for Stochastic Target in Noise

In the absence of signal-dependent clutter, $\mathbf{c}(t) = 0$ results in the special case of a noise-only scenario where the approximate information rate simplifies to

$$\dot{I}(\mathbf{y}(t);\mathbf{h}(t) \mid x(t)) = \int_W \ln\left[1 + \frac{|X(f)|^2\sigma_H^2(f)}{T_y S_{nn}(f)}\right] df. \tag{39}$$

For MI-based waveform design under the special case of a stochastic target in additive Gaussian noise, the reader is referred to [1], [2] for a detailed derivation. To quickly summarize the result based on the approach in this paper, we set $S_{cc}(f) = 0$. The mutual information (32) is then reduced to

$$\begin{aligned}\text{MI} &= I(\mathbf{y}(t);\mathbf{h}(t) \mid x(t)) \\ &= T_y \int_W \ln\left[1 + \frac{|X(f)|^2 \alpha \Upsilon_H(f)}{S_{nn}(f)}\right] df. \end{aligned} \quad (40)$$

Equation (40) is maximized with respect to $|X(f)|^2$ under the energy constraint of (3). Using the Lagrangian multiplier technique, we obtain

$$|X(f)|^2 = \max\left[0, A - \frac{S_{nn}(f)}{\alpha \Upsilon_H}\right] \quad (41)$$

where A is a constant determined by the energy constraint

$$\int_W \max\left[0, A - \frac{S_{nn}(f)}{\alpha \Upsilon_H}\right] df \le E_x.$$

Note that the function being waterfilled is the function $S_{nn}(f)/\alpha\Upsilon_H(f)$, and A defines the water level.

Finally consider the effect of substituting the definitions of α and $\Upsilon_H(f)$ back into (41) and applying the assumption $T \gg T_h$ used in [1], [2]. In this case, $\alpha\Upsilon_H(f) \to \sigma_H^2(f)/T$, and (41) becomes the same MI expression used in [1], [2]. Thus, our time-averaging interpretation of spectral variance is consistent with [1], [2].

IV. THE MI-SNR RELATIONSHIP AND TRANSMIT WAVEFORM BEHAVIOR

A. MI-SNR Relationship for Stochastic Signals

For a transmit waveform convolved with a true stochastic target in signal-dependent interference, notice that the MI rate in (29) may be rewritten in a more well-known form (Shannon's capacity equation)

$$\dot{I} = \int_W \ln(1 + \gamma(f)) df \quad (42)$$

where

$$\gamma(f) = \frac{S_{gg}(f)|X(f)|^2}{|X(f)|^2 S_{cc}(f) + S_{nn}(f)}.$$

Note, however, that $\gamma(f)$ is exactly the SINR spectral density (19) from the SNR-based design. In hindsight, the SINR spectrum needed for SNR-based transmit waveform design for stochastic targets could have been derived via inspection of (29). Nevertheless, it is satisfying to know that the SNR-based solution can be derived from another avenue, i.e., utilizing the local SNR spectrum of Kay [29].

For the extended random target case, direct inspection of (32) and (21) results in the MI-SNR relation given by

$$\text{MI} = T_y \int_W \ln\left[1 + \left\{\frac{\alpha \Upsilon_H(f)|X(f)|^2}{S_{nn}(f) + |X(f)|^2 S_{cc}(f)}\right\}\right] df \quad (43)$$

where the bracked term is clearly the SINR spectral density. In other words, MI is related to SNR via

$$\text{MI} = T_y \int_W \ln(1 + R_{\text{SINR}}(f)) df. \quad (44)$$

B. MI and SNR Transmit Waveform Behavior

In our previous work [16], we observed that in the white-noise-only case, SNR-based and MI-based waveforms form the transmit spectra differently. The SNR-based waveform tends to concentrate most of its energy in one dominant narrow frequency band while the MI-based waveform tends to distribute its energy over a few dominant frequency bands [16]. Connecting the relationship of MI to SNR for stochastic signals from the previous subsection affords us the mathematical relationship on how these waveforms are formed. We already know from (28) that the SNR-based design forms an eigenwaveform, i.e., it concentrates its energy in the primary eigenfunction which yields the dominant narrowband waveform design [16]. Now, we want to gain an insight as to why the MI-based waveform design distributes its energy to not only one but a few dominant bands. Considering the stochastic target in the white-noise-only case, the MI is given by (44) with trivially replacing $R_{\text{SINR}}(f)$ with $R_{\text{SNR}}(f)$. Then we can rewrite the MI expression to be

$$\text{MI} = T_y \int_W \text{MI}(f) df$$

where $\text{MI}(f)$ may be thought of as MI spectral density and is given by

$$\text{MI}(f) = \ln[1 + R_{\text{SNR}}(f)]. \quad (45)$$

Clearly the MI spectral density is a function of the SNR spectral density. Consider how the frequency coefficients of the MI spectral density are formed. First the MI spectral density is always nonnegative due to the addition of one to the SNR spectral density. For frequency components with small coefficients in (45), the MI spectral density is approximately equal to the SNR spectral density via Taylor series approximation. However for frequencies with large coefficients, the MI spectral density is approximately the logarithm of the SNR spectral density. The logarithm function lowers the values of these large coefficients. This effect allows for less dominant frequency components in the MI spectral density to be somewhat significant. Thus when MI-based waveforms are formed, these frequency components are allocated some energy via the waterfilling action.

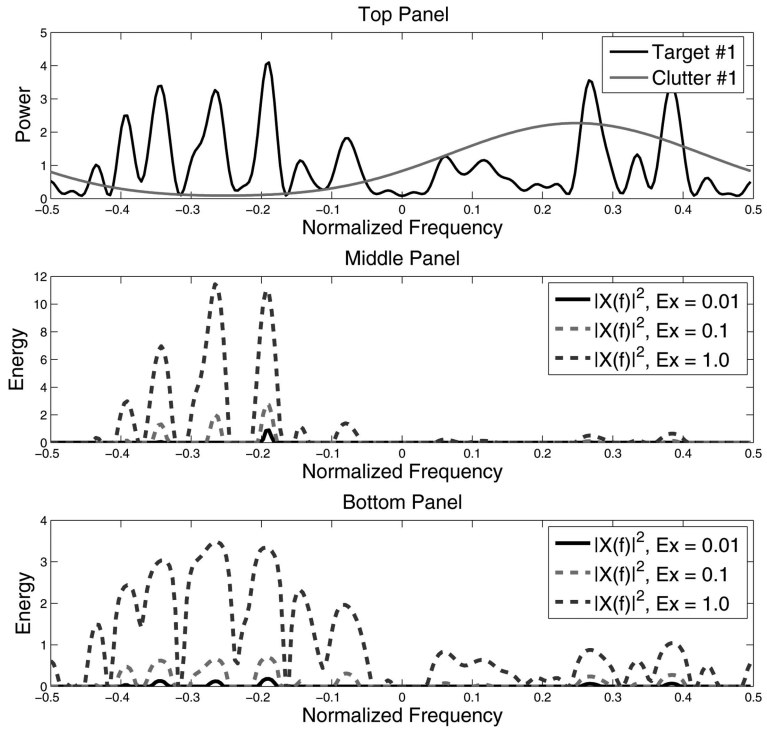

Fig. 3. Top panel: Target and clutter spectra. Middle panel: SNR-based waveform design. Bottom Panel: MI-based waveform design.

For waveform design in signal-dependent interference, the waveform behavior for SNR-based and MI-based designs are modified to account for clutter. The clutter compensating nature and the colored noise whitening effects of the waterfilling solutions for both waveforms allow the waveforms to de-emphasize frequency components where clutter is strong and emphasize where clutter power is low [18]. Consider an example given in the top panel of Fig. 3 with arbitrary target spectrum, clutter spectrum, and white noise. The middle panel of Fig. 3 shows SNR-based waveforms, and the bottom panel of Fig. 3 shows MI-based waveforms for increasing transmit energy constraints. For the low energy constraint of $E_s = 0.01$ energy units, the SNR-based waveform basically fills the dominant frequency band while the MI-based waveform distributes the energy over a few bands as expected. The signal-dependent interference has little effect on the formation of these waveforms because the system is not clutter limited. For intermediate energy of $E_s = 0.1$ units, both waveforms start to compensate for clutter while for high transmit energy $E_s = 1.0$ units, the clutter whitening action is more evident, i.e., both waveforms place most of their energy where clutter power is low.

V. EXAMPLES AND APPLICATIONS

A. SNR-Based Examples

1) *Known Target in Signal-Dependent Interference*: In this subsection, we investigate the performance of the optimum SNR-based waterfilling waveform (4) in signal-dependent interference. For a known target energy spectrum, clutter PSD, and noise PSD, it is straightforward to calculate the optimum waveform and the SINR performance (2) for various energy constraints. The resulting optimum waveform is very much dependent on all three spectra and the energy constraint. For a given energy constraint, the SINR performance changes with a change in any of these three spectra. Thus to present a performance curve, we perform a Monte Carlo simulation over different target energy spectra while holding the clutter and noise PSDs fixed. We consider 1000 different complex-valued known targets with approximately bandpass-shaped spectra. The clutter PSD has a cosine-shaped lowpass spectrum, and the noise is additive white Gaussian noise (AWGN). To define power ratios, we calculate a target's power spectrum by dividing its energy spectrum with its time duration. As such, the TNR (target-to-noise ratio) can be defined as the area under the resulting target power spectrum to the area under the noise PSD. CNR (clutter-to-noise ratio) is strictly the area ratio under the PSDs. The TNR and CNR are set to 0 dB. For each target spectrum we calculate the corresponding optimum waveform and SINR while varying the energy constraint from $E_x = 0.001$ to 100. We then average SINR over the 1000 targets. For comparison, the same simulation scheme is performed for the noise-only waveform for deterministic targets (8) as well as for a wideband (flat spectrum) impulse waveform. Note that the latter two waveforms are not clutter compensated. The results are shown in Fig. 4.

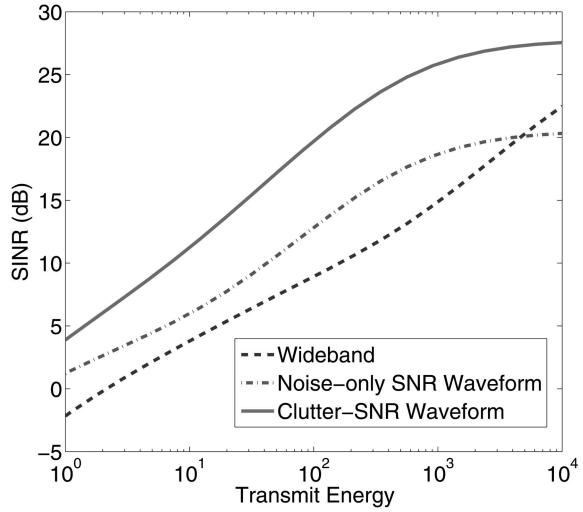

Fig. 4. SINR performances of clutter-compensating SNR-based, noise-only SNR-based, and wideband waveforms for known target in signal-dependent interference.

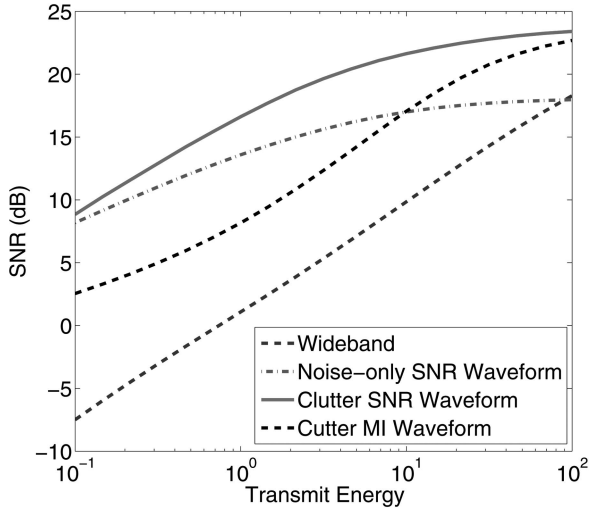

Fig. 5. SINR performances of clutter-compensating SNR-based, clutter-compensating MI-based, noise-only SNR-based, and wideband waveforms for stochastic target in signal-dependent interference.

As expected the SNR-based, clutter-compensated waveform outperforms the noise-only SNR-based waveform and the wideband impulse waveform since the former is optimized for signal-dependent interference. It is interesting to note, however, that the impulse waveform outperforms the noise-only SNR-based waveform when the transmit waveform energy is high, i.e., where the system is extremely clutter limited. In fact, the impulse waveform approaches the SINR plateau of the optimum waveform in this energy-rich regime. This is due to the fact that at high energy, the system is clutter limited and while the optimum waveform places all of its energy into narrowbands such that SINR is maximum, additional energy scales the target power and clutter power by approximately the same amount; hence, output SINR saturates. The impulse waveform eventually reaches this saturation point but at a slower rate than the optimum waveform. Since the noise-only SNR-based waveform does not compensate for clutter, it continues to place energy into frequency bands where the target response is strong, but the clutter may also be strong. Hence the noise-only SNR-based waveform converges to a lower SINR plateau at high transmit energy.

2) *Stochastic Target in Signal-Dependent Interference*: In this subsection, we investigate the SINR performance of the SNR-based waterfilling waveform (23) in signal-dependent interference for stochastic targets. The performance is compared to the performance of the MI-maximizing waveform (33) in signal-dependent interference, the noise-only SNR-based waveform (28) for stochastic targets, and a wideband impulse waveform. As in the previous subsection, for a given energy constraint, it is straightforward to calculate the average SINR performance using (22) for a given target ESV, clutter PSD, and noise PSD. Hence we again perform a Monte Carlo simulation over different target properties while holding the clutter and noise PSDs fixed. We consider 1000 wideband target ESVs. The clutter PSD has a comb-shaped spectrum, and the noise is AWGN. The TNR and CNR ratios are set to 0 dB. For each target ESV we calculate the corresponding optimum waveform and SINR while varying the energy constraint. We then average the SINR performance over the 1000 target ESVs. The results are shown in Fig. 5.

As expected the clutter-compensating SNR-based waveform outperforms the noise-only SNR-based waveform, the wideband impulse waveform, and the MI-maximizing waterfilling waveform. Three of the four waveforms converge to the same SINR plateau when the system is extremely clutter limited with the noise-only SNR-based waveform saturating earlier. Surprisingly the MI-maximizing waveform, having not been optimized for SNR, performs well for low-energy (not shown in figure) and high-energy constraints with performance degradation in an intermediate energy regime. The impulse waveform performed the poorest compared with the other three waveforms.

B. MI-Based Examples

1) *Stochastic Target in Signal-Dependent Interference*: In this subsection, we investigate the MI-extraction performance of the optimum MI waveform (33) in signal-dependent interference. This performance is compared to the MI-extraction performance of the SNR-based waterfilling waveform (23), the noise-only MI-maximizing waveform (41), and a wideband impulse waveform. For a given energy constraint, target class ESV, clutter PSD, and

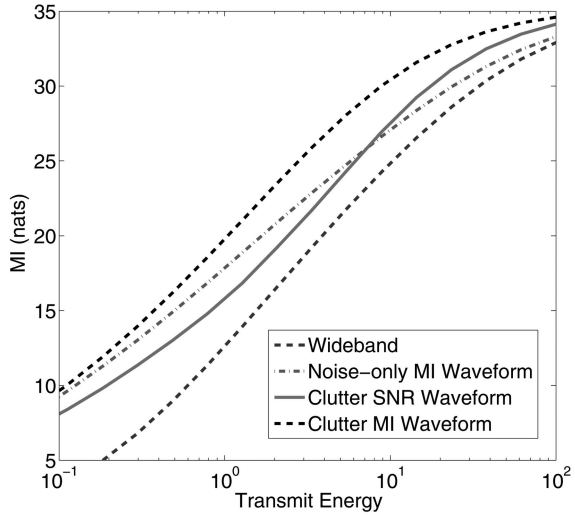

Fig. 6. MI performances of clutter-compensating MI-based, clutter-compensating SNR-based, noise-only MI-based, and wideband waveforms for stochastic target in signal-dependent interference.

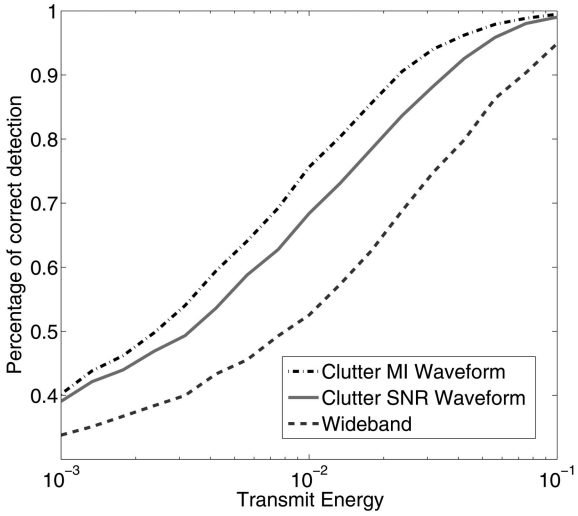

Fig. 7. Detection performances of MI-based and SNR-based waterfilling waveforms in target recognition application.

noise PSD, we can calculate the approximate MI from (32) for any of these four waveforms. We again perform a Monte Carlo simulation over 1000 target ESVs while holding the clutter and noise PSDs fixed. The targets have approximately bandpass-shaped ESVs, the noise is AWGN, and the clutter has a comb-shaped PSD. The TNR and CNR are set at 0 dB.

As shown in Fig. 6, the MI-maximizing waveform for signal-dependent interference outperforms the noise-only MI-maximizing waveform, the wideband impulse waveform, and the SNR-based waveform for signal-dependent interference. As in the previous subsection, it is noteworthy to mention that the clutter-whitening SNR-based waveform performs well in low- and high-energy regimes despite the fact that it was optimized for SNR rather than MI. The wideband impulse waveform performed the poorest in extracting mutual information.

C. Application to Ensembles with Finite Number of Hypotheses

In this subsection, we apply the waveform results derived above to two problems in target recognition or system identification. In the first experiment, our goal is to determine which target is present from among four known, deterministic alternatives. In the second experiment we again have four hypotheses, but in this case each hypothesis represents an ensemble of possibilities characterized by a known ESV. We use the idea of spectral variance to characterize the set of four hypotheses. We then evaluate detection performances of the different waveforms.

1) *Finite Number of Known Impulse Responses*: In this example, we apply the clutter-compensating SNR-based (23) and MI-based (33) waveforms in a target recognition problem. There are four hypotheses for the target channel, and each hypothesis is characterized by a known, deterministic impulse response and a prior probability of that hypothesis being true. Our goal is to identify the correct hypothesis as accurately as possible with a single, energy-limited transmission. We assume equal prior probabilities for each target, but we show how other priors could be incorporated. Since there are $M = 4$ targets, it may be a reasonable strategy to form the optimum waveform as dictated by (4) for each target impulse and to combine the resulting waveforms into one transmit pulse. However it is not clear how such a strategy should be implemented. Instead we continue with the notion of spectral variance by applying the definition of variance to the ensemble of four transfer functions. This yields an ESV function according to

$$\sigma_H^2(f) = \sum_{i=1}^{M} P_i |H_i(f)|^2 - \left| \sum_{i=1}^{M} P_i H_i(f) \right|^2 . \qquad (46)$$

Along with the energy constraint, clutter, and noise spectra, the resulting ESV function is used to form the transmit waveform. The known targets have approximately bandpass-shaped spectra. The clutter is cosine-shaped, and noise is AWGN. In this experiment, the true hypothesis is randomly chosen from a set of four known targets. Both TNR and CNR are set at 0 dB. After a single transmission a decision is made as to which target is true. The experiment is executed over a Monte Carlo of 10000 independent target set, noise, and clutter realizations. The experiment is repeated over increasing energy constraints. Fig. 7 shows the performances of the three waveforms in recognizing the true target in terms of percentage of correct decision. As one would expect, the clutter-whitening waveforms (the MI-based and SNR-based) have better detection performance

than the wideband impulse waveform. The MI-based waveform performs slightly better than the SNR-based waveform.

2) *Finite Number of Target Classes*: In this subsection, we again apply the clutter-whitening SNR-based (23) and MI-based (33) waveforms to problems in target class discrimination. Again there are four hypotheses for the target channel with each hypothesis representing a target class. Each class represents a Gaussian target ensemble described by a PSV. The top panel of Fig. 8 shows the four target PSVs for the four hypotheses in which each PSV has a bandpass shape, but each is centered in a different frequency. It is our goal to identify which target ensemble the target realization belongs to in a single transmission. We assume equal probability for $M = 4$ target ensembles. Again we utilize the idea of probability-weighted spectral variance, which is given by the ESV function

$$\sigma_H^2(f) = \sum_{i=1}^{M} Pr(H_i)\sigma_i^2(f) - \left| \sum_{i=1}^{M} Pr(H_i)\sqrt{\sigma_i^2(f)} \right|^2. \tag{47}$$

The aggregate PSV is shown in the top panel of Fig. 8. Notice that the aggregate PSV incorporates the different target hypotheses in its spectrum. The clutter is cosine-shaped, and noise is AWGN. TNR is set at 10 dB, and CNR is set at 0 dB. For each Monte Carlo trial a target class is randomly chosen from which a target realization is generated. Independent clutter and noise realizations are also generated. After one transmission a decision is made as to which ensemble the target realization belongs. Ten thousand Monte Carlo trials are performed for each energy constraint with the percentage of correct decision calculated. The detection performances of the two waveforms mentioned above along with the wideband impulse waveform are shown in the bottom panel of Fig. 8. It is interesting that the results follow the pattern of results from the target recognition experiment of the previous subsection. The clutter-compensating MI-based and SNR-based waveforms outperform the wideband impulse waveform. In this experiment, the MI-based and SNR-based waveform detection performances are very close.

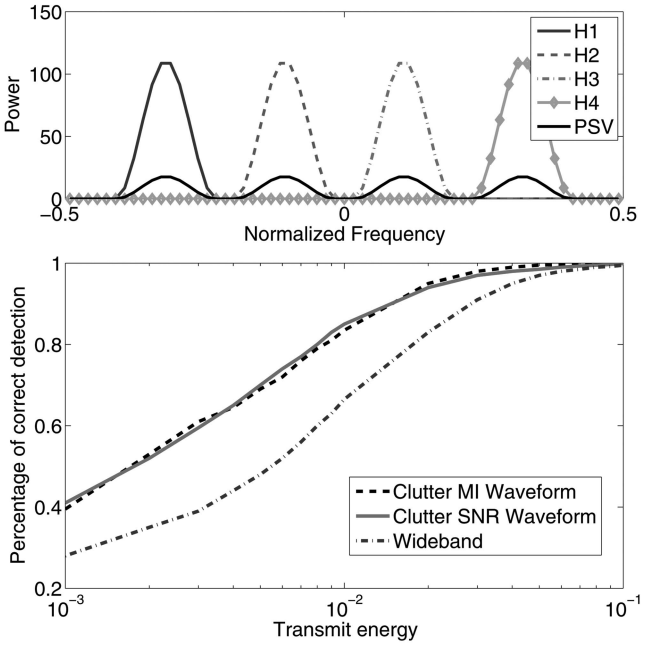

Fig. 8. Detection performances of MI-based and SNR-based waterfilling waveforms in target class discrimination application.

VI. SUMMARY AND CONCLUSIONS

A comprehensive treatment of transmit/receive waveform design matched to known or stochastic extended targets has been presented. A formalized treatment of the finite-duration random target model was also presented, with the result being a connection between finite-duration random targets and true random processes via a time-averaged spectral variance function. We used this spectral variance function to derive matched waveforms for several new scenarios.

For a known target, waveform designs were derived for two possible paradigms:

1) SNR-based waveform design in signal-dependent interference;
2) SNR-based waveform design in noise.

Our approach for optimizing SNR for a deterministic target in signal-dependent interference leads to a new solution where the numerical search required to define the waveform is over a single variable.

For a finite-duration random target, waveform designs were derived for four possible paradigms:

1) SNR-based waveform design in signal-dependent interference;
2) SNR-based waveform design target in noise;
3) MI-based waveform design in signal-dependent interference;
4) MI-based waveform design in noise.

The derivations for SNR-based stochastic target optimization are new results. For both MI-based designs, the optimum transmit waveforms turned out to be waterfilling solutions in the frequency domain. The waveform for MI-based optimization in signal-dependent interference is a new result. In terms of waveform design for stochastic targets, connections between MI and SNR have been discussed.

Numerous examples were conducted to show performances of optimum waveforms in various paradigms. We evaluated the waveforms in terms of the SNR and MI metrics used to derive the waveforms as well as for a target recognition application for a finite number of target hypotheses.

APPENDIX I. DERIVATION OF SNR-BASED WATERFILLING WAVEFORM FOR KNOWN TARGET IN SIGNAL-DEPENDENT INTERFERENCE

THEOREM 1 *The $|X(f)|^2$ that maximizes the SINR equation given by*

$$(\text{SINR})_{t_0} = \int_W \frac{|H(f)|^2|X(f)|^2}{S_{cc}(f)|X(f)|^2 + S_{nn}(f)}df. \tag{48}$$

given the constraint

$$E_x \geq \int_W |X(f)|^2 df \tag{49}$$

is

$$|X(f)|^2 = \max[0, B(f)(A - D(f))] \tag{50}$$

where $B(f)$ and $D(f)$ are described by the following equations

$$B(f) = \frac{\sqrt{|H(f)|^2 S_{nn}(f)}}{S_{cc}(f)} \tag{51}$$

$$D(f) = \sqrt{\frac{S_{nn}(f)}{|H(f)|^2}}. \tag{52}$$

PROOF We invoke the Lagrangian multiplier technique yielding an objective function

$$K(|X(f)|^2, \lambda) = \int_W \frac{|H(f)|^2|X(f)|^2}{S_{cc}(f)|X(f)|^2 + S_{nn}(f)}df + \lambda\left[E_x - \int_W |X(f)|^2 df\right]. \tag{53}$$

This is equivalent to maximizing $k(|X(f)|^2)$ with respect $|X(f)|^2$ where $k(|X(f)|^2)$ is given by

$$k(|X(f)|^2) = \frac{|H(f)|^2|X(f)|^2}{S_{cc}(f)|X(f)|^2 + S_{nn}(f)}df - \lambda|X(f)|^2. \tag{54}$$

Taking the derivative of $k(|X(f)|^2)$ with respect to $|X(f)|^2$ and setting it to zero yields the $|X(f)|^2$ that maximizes (48), where $|X(f)|^2$ is given by

$$|X(f)|^2 = -\frac{S_{nn}(f)}{S_{cc}(f)} \pm \sqrt{\frac{S_{nn}(f)|H(f)|^2}{\lambda S_{cc}^2(f)}}. \tag{55}$$

Setting $A = 1/\sqrt{\lambda}$, rearranging terms, and ensuring $|X(f)|^2$ to be positive, the $|X(f)|^2$ that maximizes SINR is given by

$$|X(f)|^2 = \max\left[0, \frac{\sqrt{|H(f)|^2 S_{nn}(f)}}{S_{cc}(f)}\left(A - \sqrt{\frac{S_{nn}(f)}{|H(f)|^2}}\right)\right]. \tag{56}$$

APPENDIX II. DERIVATION OF MI-BASED WATERFILLING WAVEFORM IN SIGNAL-DEPENDENT INTERFERENCE

THEOREM 2 *The $|X(f)|^2$ that maximizes the mutual information*

$$I(\mathbf{y}(t); \mathbf{h}(t) \mid x(t)) = T_y \int_W \ln\left[1 + \frac{|X(f)|^2 \alpha \Upsilon_H(f)}{S_{nn}(f) + |X(f)|^2 S_{cc}(f)}\right] df \tag{57}$$

is given by

$$|X(f)|^2 = \max\left[0, -R(f) + \sqrt{R^2(f) + S(f)(A - D(f))}\right] \tag{58}$$

where $D(f)$, $R(f)$, and $S(f)$ are defined by (34)–(36).

PROOF We invoke the Lagrangian multiplier technique yielding an objective function

$$K(|X(f)|^2, \lambda) = T_y \int_W \ln\left[1 + \frac{|X(f)|^2 \alpha \Upsilon_H(f)}{S_{nn}(f) + |X(f)|^2 S_{cc}(f)}\right] df + \lambda\left[E_x - \int_W |X(f)|^2 df\right]. \tag{59}$$

This is equivalent to maximizing $k(|X(f)|^2)$ with respect $|X(f)|^2$ where $k(|X(f)|^2)$ is given by

$$k(|X(f)|^2) = T_y \ln\left[1 + \frac{|X(f)|^2 \alpha \Upsilon_H(f)}{S_{nn}(f) + |X(f)|^2 S_{cc}(f)}\right] - \lambda|X(f)|^2. \tag{60}$$

Taking the derivative of $k(|X(f)|^2)$ with respect to $|X(f)|^2$ and setting it to zero yields

$$\frac{\lambda}{T_y} = \frac{S_{nn}(f)\alpha \Upsilon_H(f)}{A(f)|X(f)|^4 + B(f)|X(f)|^2 + C(f)} \tag{61}$$

where $A(f)$, $B(f)$, and $C(f)$ are given by the following;

$$A(f) = S_{cc}(f)(S_{cc}(f) + \alpha \Upsilon_H(f)) \tag{62}$$

$$B(f) = S_{nn}(f)(2S_{cc}(f) + \alpha \Upsilon_H(f)) \tag{63}$$

and

$$C(f) = S_{nn}^2(f). \tag{64}$$

Setting $A = T_y/\lambda$ and ensuring $|X(f)|^2$ to be positive, the $|X(f)|^2$ that maximizes the mutual information is given by

$$|X(f)|^2 = \max\left[0, -R(f) + \sqrt{R^2(f) + S(f)(A - D(f))}\right]. \tag{65}$$

REFERENCES

[1] Bell, M. R.
Information theory and radar waveform design.
IEEE Transactions on Information Theory, **39**, 5 (Sept. 1993), 1578–1597.

[2] Bell, M. R.
Information theory and radar: Mutual information and the design and analysis of radar waveforms and systems.
Ph.D. dissertation, California Institute of Technology, 1988.

[3] Pillai, S., Oh, H., Youla, D., and Guerci, J.
Optimum transmit-receiver design in the presence of signal-dependent interference and channel noise.
IEEE Transactions on Information Theory, **46**, 2 (Mar. 2000), 577–584.

[4] Kay, S.
Optimal signal design of Gaussian point targets in stationary Gaussian clutter/reverberation.
IEEE Journal of Selected Topics in Signal Processing, **1**, 1 (June 2007), 31–41.

[5] Guerci, J. R. and Pillai, S. U.
Theory and application of optimum transmit-receive radar.
In *Proceedings of the IEEE 2000 International Radar Conference*, Washington, D.C., May 8–12, 2000, 705–710.

[6] Garren, D. A., Osborn, M. K., Odom, A. C., Goldstein, J. S., and Guerci, J. R.
Enhanced target detection and identification via optimised radar transmission pulse shape.
IEE Proceedings—Radar, Sonar and Navigation, **148**, 3 (June 2001), 130–138.

[7] Esposito, R. and Schumer, M.
Probing linear filters—signal design for the detection problem.
IEEE Transactions on Information Theory, **16**, 2 (Mar. 1970), 167–171.

[8] Mosca, E.
Probing signal design for linear channel identification.
IEEE Transactions on Information Theory, **18**, 4 (July 1972), 481–487.

[9] Gjessing, D. T.
Target Adaptive Matched Illumination Radar Principles and Applications.
New York: Peregrinus, Ltd., 1986.

[10] DeLong, J. D. F. and Hofstetter, E. M.
On the design of optimum radar waveforms for clutter rejection.
IEEE Transactions on Information Theory, **IT-13**, 3 (July 1967), 454–463.

[11] Sowelam, S. M. and Tewfik, A. H.
Waveform selection in radar target classification.
IEEE Transactions on Information Theory, **IT-13**, 3 (July 1967), 454–463.

[12] Guo, D., Shamai, S., and Verdu, S.
Mutual information and minimum mean-square error in Gaussian channels.
IEEE Transactions on Information Theory, **51**, 4 (Apr. 2005), 1261–1282.

[13] Yang, Y. and Blum, R. S.
MIMO radar waveform design based on mutual information and minimum mean-square error estimation.
IEEE Transactions on Aerospace and Electronic Systems, **43**, 1 (Jan. 2007), 330–343.

[14] Leshem, A., Naparstek, O., and Nehorai, A.
Information theoretic adaptive radar waveform design for multiple extended targets.
IEEE Journal of Selected Topics in Signal Processing, **1**, 1 (June 2007), 42–55.

[15] Haykin, S.
Cognitive radar: A way of the future.
IEEE Signal Processing Magazine, **23**, 1 (Jan. 2006), 30–40.

[16] Goodman, N. A., Venkata, P. R., and Neifeld, M. A.
Adaptive waveform design and sequential hypothesis testing for target recognition with active sensors.
IEEE Journal of Selected Topics in Signal Processing, **1**, 1 (June 2007), 105–113.

[17] Bae, J. and Goodman, N.
Adaptive waveforms for target class discrimination.
In *Proceedings of the 2007 Waveform Diversity and Design Conference*, Pisa, Italy, June 2007, 395–399.

[18] Romero, R. and Goodman, N.
Information theoretic matched waveform in signal dependent interference.
In *Proceedings of the 2008 IEEE Radar Conference* (RADAR '08), Rome, Italy, May 26–30, 2008.

[19] Pillai, S., Li, K. Y., and Beyer, H.
Waveform design optimization using bandwidth and energy considerations.
In *Proceedings of the 2008 IEEE Radar Conference* (RADAR '08), Rome, Italy, May 26–30, 2008.

[20] Patton, L. and Rigling, B.
Modulus constraints in adaptive radar waveform design.
In *Proceedings of the 2008 IEEE Radar Conference* (RADAR '08), Rome, Italy, May 26–30, 2008.

[21] Pillai, S., Li, K. Y., and Beyer, H.
Reconstruction of constant envelope signals with given Fourier transform magnitude.
In *Proceedings of the 2009 IEEE Radar Conference* (RADAR '09), Pasadena, CA, May 4–8, 2009, 1–4.

[22] Papoulis, A. and Pillai, S.
Probability, Random Variables, and Stochastic Processes.
Columbus, OH: McGraw-Hill, 2002.

[23] Cover, T. M. and Thomas, J. A.
Elements of Information Theory.
Hoboken, NJ: Wiley, 1991.

[24] Lathi, B. P.
Linear Systems and Signals.
Carmichael, CA: Berkeley-Cambridge Press, 1992.

[25] Miller, K. S.
Complex Stochastic Processes.
Reading, MA: Addison-Wesley, 1974.

[26] Doob, J. L.
Stochastic Processes.
Hoboken, NJ: Wiley, 1953.

[27] Peebles, P. Z.
Probability, Random Variables, and Random Signal Principles (3rd ed.).
Columbus, OH: McGraw-Hill, 1993.

[28] Helstrom, C. W.
Statistical Theory of Signal Detection (2nd ed.).
Elmsford, NY: Pergamon, 1968.

[29] Kay, S.
Fundamentals of Statistical Signal Processing, vol. I: *Estimation Theory.*
Upper Saddle River, NJ: Prentice-Hall, 1993.

Ric A. Romero (S'07—M'10) received his Ph.D. in electrical and computer engineering from the University of Arizona in 2010, his M.S.E.E. degree from the University of Southern California in 2004 and his B.S.E.E. from Purdue University in 1999. He is currently pursuing a doctoral degree in electrical engineering at the University of Arizona.

From 1999–2010, he was a Senior Multidisciplined Engineer II at Raytheon Missile Systems in Tucson, AZ. He has been involved in various communications, radar, and research and development programs. He is also a graduate research assistant at the Laboratory for Sensor and Array Processing, University of Arizona from 2007 through 2010. He is currently an assistant professor in the Department of Electrical and Computer Engineering, Naval Postgraduate School, Monterey, CA. His research interests are in the general areas of radar, sensor information processing, and communications.

Dr. Romero was awarded the 2004 Corporate Excellence in Technology Award, a company-wide technical prize at Raytheon Corporation. He was also granted the Raytheon Advanced Scholarship Program fellowships from 2002–04 and 2005–07.

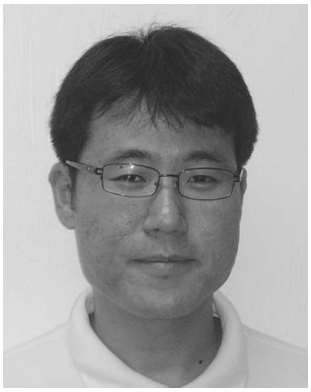

Junhyeong Bae (S'09) received the B.S. degree from Kyungpook National University, South Korea in 2005 and the M.S. degree in electrical and computer engineering from the University of Arizona, Tucson in 2008.

He is currently pursuing the Ph.D. degree in electrical and computer engineering at the University of Arizona. He is a graduate research assistant at the Laboratory for Sensor and Array Processing (LSAP). His research interests include radar and array signal processing.

Nathan A. Goodman (S'98—M'02—SM'07) received the B.S., M.S., and Ph.D. degrees in electrical engineering from the University of Kansas, Lawrence, in 1995, 1997, and 2002, respectively.

From 1996 to 1998, he was an RF Systems Engineer for Texas Instruments, Dallas, TX. From 1998 to 2002, he was a graduate research assistant in the Radar Systems and Remote Sensing Laboratory, University of Kansas. He is currently an associate professor in the Department of Electrical and Computer Engineering, University of Arizona, Tucson. Within the department, he directs the Laboratory for Sensor and Array Processing. His research interests are in radar and array signal processing.

Dr. Goodman was awarded the Madison A. and Lila Self Graduate Fellowship from the University of Kansas in 1998. He was also awarded the IEEE 2001 International Geoscience and Remote Sensing Symposium Interactive Session Prize Paper Award.